Design of a NonLinear Observer for a Laboratory Antilock Braking System

Marcela Martinez-Gardea, * **Iordan J. Mares Guzmán,** *
Cuauhtémoc Acosta Lúa, * **Stefano Di Gennaro** **
Ivan Vázquez Álvarez ***

* *Centro Universitario de la Ciénega, Universidad de Guadalajara, Ocotlán, Jalisco, Mexico*
(e-mail: {marcela.martinezg, iordan.mares}@alumno.udg.mx, cuauhtemoc.acosta@cuci.udg.mx*)*

** *Department of Information Engineering, Computer Science and Mathematics Center of Excellence DEWS, University of L'Aquila Via Vetoio, Loc. Coppito, 67100 – L'Aquila, Italy*
(e-mail: stefano.digennaro@univaq.it*)*

*** *Universidad Autónoma Metropolitana, México, D.F*
(e-mail: iva@correo.azc.uam.mx*)*

Abstract: In this paper a nonlinear observer is presented in order to estimate the angular velocity of both upper and lower wheels of a PC controlled ABS Laboratory setup, from Inteco Ltd. The system simulates the dynamics of a quarter car model. In order to accomplish this, it includes two attached wheels. The angular velocity of the upper wheel simulates the angular velocity of a vehicle's wheel, while the lower wheel simulates the road surface. In the observer design, it is assumed that the angular velocity of the vehicle's wheel is known, since a sensor is installed on the system, as in a real vehicle, so that the longitudinal velocity can be determined with this information. The proposed nonlinear observer considers the Pacejka's "magic formula" to calculate the contact force. This formula allows the observer to estimate the states in both the linear and nonlinear regions. The stability of the observer is proved and validated with simulations, and experimentally with the Antilock Braking System Laboratory setup.

Keywords: Antilock braking system, Nonlinear observer, Stability.

1. INTRODUCTION

The Antilock Braking System (ABS) was developed to prevent the wheels from locking up while braking. This prevents the slippage of the wheels on the surface, adjusting the brake fluid pressure level of each wheel, and helps the driver to keep vehicle's control (Petrov et al. (1977), Rittmannsberger (1998), Emig et al. (1990)). In fact, the ABS is designed to increase the braking efficiency and to maintain the vehicle's maneuverability, reducing the driving instability and decreasing the braking distance.

Modern ABS systems try not only to prevent the wheels from locking up, but also aim to obtain maximum wheel grip on the surface while the vehicle is braking (Kiencke and Nielsen (2010), Rajamani (2011)). The technical difficulties to implement successfully the antilock concept, contained in the 1936 patent for an "apparatus for preventing lock braking of wheels in a motor vehicle" by Robert Bosch (Bosch GmbH (2003)), were solved between 1967 and 1970, when Mercedes–Benz engineers changed the mechanical sensors for contactless sensors operating under the induction principle (DaimlerAG (2008)). Finally, when the electronic integrated circuits were small and robust enough, it was possible to record data from the wheel's sensors, and to use more reliable actuators for imposing brake hydraulic pressure. The mass production started with the ABS second generation, in 1978 (DaimlerAG (2008)).

With the hardware technology breakthroughs, now the challenge is to propose efficient control algorithms for the actuators. Several algorithms had been aimed for controlling the ABS.

In this paper, a mechatronic system, an ABS Laboratory setup manufactured by Inteco Ltd, was used to obtain the mathematical model and implement the physical simulation. The setup represents a quarter car model, and it consists of two rolling wheels. The lower wheel, made of aluminum, imitates the relative road motion of the car, whereas the upper wheel, made of rigid plastic, simulates the wheel of the vehicle. In order to accelerate the lower wheel, a large DC motor is coupled to it. The upper wheel is equipped with a disk–brake system that is driven by a

⋆ Research supported by CONACYT scholarships 513153 and 512691.

small DC motor where the control input is applied (Inteco (2006)).

Earlier works on control applied to ABS Laboratory setups are mainly based on the assumption that information of all sensors is available for measurement. This assumption can be considered valid, because nowadays modern cars contain several sensors. In the literature, controller design based on nonlinear techniques can be found in Al-Mola et al. (2014), Khanesar et al. (2012), Oniz et al. (2009), John and Pedro (2009), Dadashnialehi et al. (2012) or intelligent control techniques as in Dadashnialehi et al. (2014), Kayacan et al. (2009), Precup et al. (2012), Cabrera et al. (2005), Topalov et al. (2009a,b), Precup et al. (2010a,b), Habibi and Yazdizadeh (2010), Topalov et al. (2011).

On the other hand, a nonlinear observer is applied to an ABS Laboratory setup in Chen et al. (2006) where an observer–based adaptive fuzzy neural controller is proposed and the stability is proven by the Lyapunov theory. Also, it is possible to find articles about nonlinear observers of the vehicle longitudinal velocity, as in Zhao et al. (2011), where a nonlinear observer is presented for estimating the longitudinal and lateral vehicle velocities based on Duggof's tire model and vehicle dynamics. In Imsland et al. (2007) an observer for automotive vehicle velocity estimation is presented, in the presence of varying friction and road bank angles. The same type of observer, in addition to an observer forcing the dynamics of the nonlinear estimation error to the dynamics of a linear reference system, is investigated in Kiencke and Nielsen (2010). Other types of observers, linear and nonlinear, using the sliding mode techniques are referred in Baffet et al. (2007) and Stephant et al. (2007).

The main problem considered in this work is the fact that some of the state variables, necessary to implement the previous control strategies, are usually not measured, due to sensor cost and space occupancy in the vehicle. For instance, the longitudinal velocity is rarely measured. Therefore these variables have to be estimated from the available measurements, such as the angular velocity of the wheel.

The main contributions of this work are:

1. The mathematical model of the ABS Laboratory setup was enriched by introducing Pacejka's magic formula (Pacejka (2006)), which allows the observer to work with a tire–road friction model in the linear and nonlinear regions of the system. This model, in comparison to others as (Zhao et al. (2011)), provides an accurate behavior of tire mechanics based on real experiments test data. The so–called "magic formula" contains some coefficients to be determined experimentally, so that the output is similar to the experimental tire behavior. An additional advantage of using the magic formula is its wide use in the automotive industry.
2. The development of a nonlinear observer for the longitudinal velocity of the vehicle using the available information of the ABS Laboratory setup sensors. The observer's importance relies on the fact that modern vehicles estimate the longitudinal velocity, but this estimate is no longer accurate during the braking process.
3. Simple computation of the observer's gains that implies an easy and fast implementation of the observer. For instance, a significant advantage of the proposed observer over the extended Kalman filter (Stephant et al. (2007)) is that the real–time solution of the Riccati differential equations is avoided. The proposed observer is implemented more efficiently because the gains obtained are easy for the implementation on the electronic control unit.
4. The proposed observer guarantees theoretical stability, developed through practical stability and proven by a Lyapunov function.
5. The observer is validated, through simulations, implemented and tested on the ABS Laboratory setup.

The paper is organized as follows: Section 2 briefly presents the development of a mathematical model of the experimental ABS Laboratory setup. Section 3 is dedicated to the observer design and the demonstration of the asymptotic stability provided by the error feedback using Lyapunov function techniques. The result and discussion are shown in Section 4. Finally, in the last Section, the conclusion is presented.

2. MATHEMATICAL MODEL OF THE EXPERIMENTAL ABS LABORATORY SETUP

As mentioned, the Laboratory setup by Inteco Ltd. considered in this paper consists of two rolling wheels, see Fig. 1. Although simple, it preserves the fundamental characteristics of an actual ABS system (Inteco (2006)). The Inteco Ltd. ABS Laboratory setup characterizes a vehicle's ABS in the range 0–70 km/h, allows testing control and observer algorithms, and can be easily adapted for a real implementation.

The angular velocity of the upper wheel corresponds to the angular velocity of the vehicle's wheel (Inteco (2006)). In addition, with the ABS Laboratory setup, it is possible to simulate the road surface through the lower wheel. The *control problem* is to maintain the wheel slip at a reference desired value. The wheel slip describes the normalized difference between the velocities of both wheels. The setup is equipped with identical encoders on the wheels that allow determining the wheel slip. These encoders provide the wheel angular positions, with a measurement accuracy of $2\pi/4096 = 0.0015$ rad, and the wheel angular velocities, through differential quotients.

Nowadays, an actual vehicle estimates the longitudinal velocity applying a relationship between the angular velocity of the wheel and the wheel's radius, considering the wheels deformation very small compared to the wheel's dimensions. This estimation is good, as long as no slip is present. Unfortunately, the braking process involves slip between the wheel and the road surface. When it occurs, it is not possible to estimate the longitudinal velocity in the same way. This motivates the design of an observer capable of estimating this variable. The encoder on the lower wheel allows a direct measurement of the longitudinal velocity. This information will be used in order to validate the observer's results when is applied on a real vehicle.

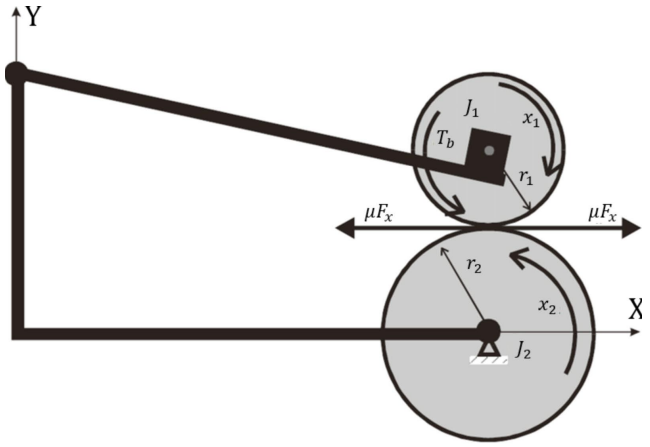

Fig. 1. Scheme of the ABS Laboratory setup.

2.1 Mathematical Model

The mathematical model of the ABS Laboratory setup is derived under the following assumptions. First, the lateral and the vertical motions are neglected. Second, the rolling resistance force is ignored, as it is very small due to braking (see Fig.2).

The braking torque, T_b, and the bearing friction torque, M_{10}, act on the upper wheel. The bearing friction torque, M_{20}, acts on the lower wheel. The tractive force, F_x, acts on both, the upper and lower wheels. The dynamic equations of the ABS Laboratory setup are (Inteco (2006))

$$\begin{aligned} \dot{x}_1 &= \frac{r_1}{J_1} F_x s - \frac{1}{J_1}(d_1 x_1 + M_{10} + T_b) s_1 \\ \dot{x}_2 &= -\frac{r_2}{J_2} F_x s - \frac{1}{J_2}(d_2 x_2 + M_{20}) s_2 \end{aligned} \tag{1}$$

where x_1, x_2 are the angular velocities of the upper and lower wheels, whose inertia moments are J_1, J_2 and whose radii are r_1, r_2. Furthermore, d_1, d_2 are the viscous friction coefficients of the upper and lower wheel and $s(x), s_1(x_1)$ and $s_2(x_2)$ are auxiliary variables

$$\begin{aligned} s(x) &= \text{sign}(r_2 x_2 - r_1 x_1) \\ s_1(x_1) &= \text{sign}(x_1) \\ s_2(x_2) &= \text{sign}(x_2) \end{aligned}$$

used to determinate if the vehicle is in the traction mode or in the braking mode, with

$$\text{sign}(x) = \begin{cases} 1 & \text{if } x > 0 \\ 0 & \text{if } x = 0 \\ -1 & \text{if } x < 0. \end{cases}$$

Moreover, instead of building the mathematical model with the physical parameters of the ABS setup, the Pacejka's magic formula was chosen to describe the tractive dynamics. The magic formula approximates the tire characteristic curve, and is based on empirical measurements. It is widely used in tire's dynamic works and allows working with a wider range of values, including the linear and nonlinear regions of the tire characteristic

$$F_x = \mu D_x \sin\Big(C_x \arctan(B_x \lambda)\Big) \tag{2}$$

where the positive experimental coefficients, given by the stiffness factor B_x, the shape factor C_x, and the peak value D_x, are determined to match the experimental data,

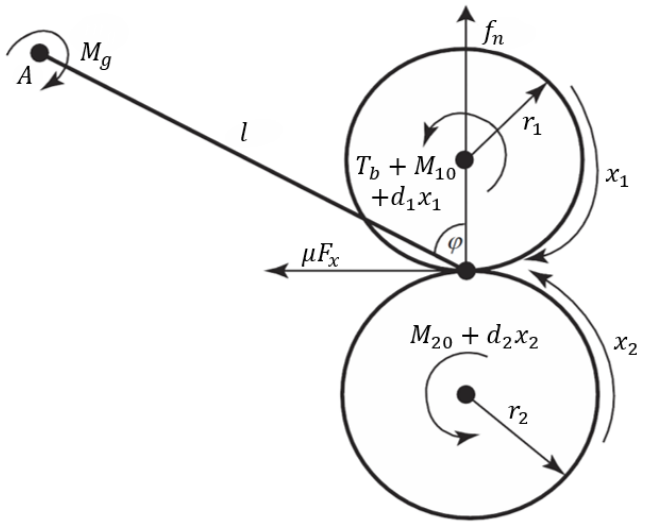

Fig. 2. Forces and torques acting in the ABS Laboratory setup.

$\mu \in [0, 1]$ is the friction coefficient between the upper and lower wheel and F_x is the tractive force, i.e. the force used to generate motion between a body and a tangential surface.

An advantage of the Pacejka model is that it is based on trigonometrical functions and, as mentioned, relies on experimental coefficients tuned so that the output fits the experimental results. Fig. 3 shows the behavior of the tractive force calculated in (2).

Finally, the equation (2) depends on the wheel slip function

$$\lambda = \frac{r_2 x_2 - r_1 x_1}{r_2 x_2} \tag{3}$$

i.e. of the relative difference of the wheel velocities.

The braking torque, T_b, is modeled by a first–order equation (Inteco (2006)), given by

$$\dot{T}_b = -c_{31} T_b + c_{31} b(u) \tag{4}$$

where c_{31} is a constant, and $b(u)$ describes the relation between the control input applied to the DC motor, which drives the action of the brake pads, with the control input $u \in [0, 1]$, and generates the braking torque T_b. This relation can be approximated by

$$b(u) = \begin{cases} b_1 u + b_2 & \text{if } u \geq u_0 \\ 0 & \text{if } u < u_0 \end{cases} \tag{5}$$

where b_1, b_2 are constants. T_b is applied by the brake pad to the rotor attached to the upper wheel (the upper wheel in the setup emulates the behavior of the tire in the car), however, that force is generated by the control signal u, the voltage applied to the DC motor. Since the brake dynamic is fast compared with the wheels' dynamics, (4) can be approximated as follows

$$T_b = b_1 u + b_2. \tag{6}$$

The control of the ABS can be obtained calculating T_b (Al-Mola et al. (2014), Dadashnialehi et al. (2014), Khanesar et al. (2012), Precup et al. (2012), Kayacan et al. (2009), Oniz et al. (2009)), and u can be easily calculated with (6), since b_1 and b_2 are known.

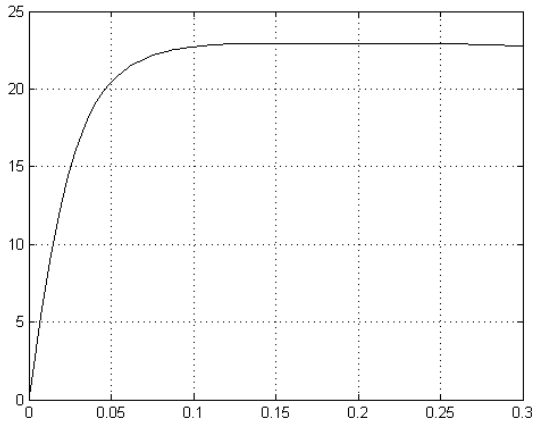

Fig. 3. Tractive force F_x vs wheel slip λ.

Under normal operation conditions, the velocity r_1x_1 matches the forward velocity r_2x_2. When the brake is applied, braking forces are generated at the wheel interface, so r_1x_1 will tend to be lower than v_x, and a slippage will occur.

In the following section an observer for $\hat{x}_2$ will be designed, assuming that the variable state x_1 is measurable through an encoder, and the disturbance M_{10}, M_{20} can be calculated.

In this article it is assumed that the brakes are applied (Al-Mola et al. (2014); Dadashnialehi et al. (2014); Khanesar et al. (2012); Precup et al. (2012); Kayacan et al. (2009); Martinez-Gardea et al. (2014)), and a braking force is generated because of the interaction of the two wheels, which cause the wheel slip λ to increase. As the braking force increases, a slippage will occur between the tire and the road surface, and the wheel speed will tend to be lower than the vehicle speed.

In this situation the values of the auxiliary variables, s, s_1 and s_2 are the following

$$\begin{aligned} s &= \text{sign}(r_2x_2 - r_1x_1) = 1 \\ s_1 &= \text{sign}(x_1) = 1 \\ s_2 &= \text{sign}(x_2) = 1. \end{aligned} \tag{7}$$

Considering (7), equations (1) can be rewritten as

$$\begin{aligned} \dot{x}_1 &= \frac{r_1}{J_1}F_x - \frac{1}{J_1}(d_1x_1 + M_{10} + T_b) \\ \dot{x}_2 &= -\frac{r_2}{J_2}F_x - \frac{1}{J_2}(d_2x_2 + M_{20}). \end{aligned} \tag{8}$$

3. OBSERVER DESIGN

The proposed nonlinear observer is a simple Luenberger–like observer based on a copy of the system (8)

$$\begin{aligned} \dot{\hat{x}}_1 &= \frac{r_1}{J_1}\hat{F}_x - \frac{1}{J_1}(d_1\hat{x}_1 + M_{10} + T_b) + k_{o1}(x_1 - \hat{x}_1) \\ \dot{\hat{x}}_2 &= -\frac{r_2}{J_2}\hat{F}_x - \frac{1}{J_2}(d_2\hat{x}_2 + M_{20}) + k_{o2}(x_1 - \hat{x}_1) \end{aligned} \tag{9}$$

where k_{o1}, k_{o2} are the observer's gains. In this observer, the estimated tractive force $\hat{F}_x$ is a copy of (2), and is defined as

$$\hat{F}_x = \mu D_x \sin\Big(C_x \arctan(B_x\hat{\lambda})\Big) \tag{10}$$

where

$$\hat{\lambda} = \frac{r_2\hat{x}_2 - r_1\hat{x}_1}{r_2\hat{x}_2}. \tag{11}$$

Let us consider the estimation errors

$$\begin{aligned} e_1 &= x_1 - \hat{x}_1 \\ e_2 &= x_2 - \hat{x}_2 \end{aligned} \tag{12}$$

and their derivatives obtained from (8), (9)

$$\begin{aligned} \dot{e}_1 &= -\Big(k_{o1} + \frac{d_1}{J_1}\Big)e_1 + \frac{r_1}{J_1}(F_x - \hat{F}_x) \\ \dot{e}_2 &= -k_{o2}e_1 - \frac{d_2}{J_2}e_2 - \frac{r_2}{J_2}(F_x - \hat{F}_x). \end{aligned} \tag{13}$$

The error equations (13) can be rewritten as

$$\dot{e} = Ae + B(F_x - \hat{F}_x) \tag{14}$$

where $e = (e_1, e_2)^T$ and

$$A = \begin{pmatrix} -k_{o1} - \dfrac{d_1}{J_1} & 0 \\ -k_{o2} & -\dfrac{d_2}{J_2} \end{pmatrix} r2,\ B = \begin{pmatrix} \dfrac{r_1}{J_1} \\ -\dfrac{r_2}{J_2} \end{pmatrix}.$$

The stability of the error origin is studied using the quadratic Lyapunov candidate $V_o(e) = e^TPe/2$, with $P = P^T > 0$, whose derivative along the dynamics (14) is

$$\dot{V}_o(e) = e^T\frac{A^TP + PA}{2}e + e^TPB(F_x - \hat{F}_x).$$

Defining a constant matrix

$$Q = \begin{pmatrix} q_1 & 0 \\ 0 & q_2 \end{pmatrix} = Q^T > 0$$

and determining the values of the matrix

$$P = \begin{pmatrix} p_{11} & p_{12} \\ p_{12} & p_{22} \end{pmatrix}$$

such that

$$A^TP + PA = -2Q \tag{15}$$

one obtains

$$\begin{aligned} p_{11} &= \frac{q_1J_1d_2s_2(J_1(J_2k_{o1} + d_2s_2) + J_2d_1s_1) + q_2(J_1J_2k_{o2})^2}{d_2s_2(J_1k_{o1} + d_1s_1)(J_1J_2k_{o1} + J_1d_2s_2 + J_2d_1s_1)} \\ p_{12} &= -\frac{J_1J_2^2q_2k_{o2}}{d_2s_2\big(J_1d_2s_2 + J_1J_2k_{o1} + J_2d_1s_1\big)} \\ p_{22} &= \frac{J_2q_2}{d_2s_2}. \end{aligned} \tag{16}$$

In order to get a positive definite matrix P, one requires that all the determinants of the principal minors of P are positive

$$\begin{aligned} &\frac{J_1\big(J_1J_2^2q_2k_{o2}^2 + J_1d_2^2q_1 + q_1J_1J_2d_2 + q_1J_2d_1d_2\big)}{d_2\big(J_1^2d_2k_{o1} + J_1^2J_2k_{o1}^2 + 2J_1J_2d_1k_{o1} + d_1d_2J_1 + d_1^2J_2\big)} > 0 \\ &\frac{q_1\Big(\big(J_1J_2k_{o1} + (J_1d_2 + J_2d_1)\big)^2 + q_2\big(J_1J_2k_{o2}\big)^2\Big)}{\Big(d_2(J_1d_2 + J_1J_2ko1 + J_2d_1)^2(J_1k_{o1} + d_1)\Big)} > 0. \end{aligned} \tag{17}$$

The conditions (17) are ensured to hold true by an appropriate choice of the gains k_{o1}, $k_{o2} > 0$.

Hence, the Lyapunov function derivative can be rewritten as

$$\begin{aligned}\dot{V}_o(e) &= -\|e\|_Q^2 + e^T PB(F_x - \hat{F}_x) \\ &\leq -\lambda_{\min}^Q \|e\|_Q^2 + \|PB\|\|F_x - \hat{F}_x\|\|e\|\end{aligned} \tag{18}$$

$$\|F_x - \hat{F}_x\| = \phi(e_2, x_1, \hat{x}_1) \tag{19}$$

with $\|e\|_Q^2 = e^T Qe$, $\lambda_{\min}^Q$ the minimum eigenvalue of Q, and where ϕ is a function that tends to zero exponentially. Setting where $\Delta = \|PB\|$, it is finally possible to bound the derivative of the Lyapunov function as follows

$$\dot{V}_o(e) \leq -\lambda_{\min}^Q \|e\|_Q^2 + \Delta\phi\|e\|. \tag{20}$$

To prove the square integrability of $e(t)$, let us integrate both sides of (20)

$$\begin{aligned}V_o\,|_{t,x} - V_o\,|_{t_0,x_0} &\leq -\lambda_{\min}^Q \int_{t_0}^{t} \|e(\tau)\|^2 d\tau \\ &\quad + \Delta \int_{t_0}^{t} \|\phi(\tau)\|\|e(\tau)\| d\tau \\ &\leq -\lambda_{\min}^Q \int_{t_0}^{t} \|e(\tau)\|^2 d\tau \\ &\quad + \Delta \left[\int_{t_0}^{t} \|\phi(\tau)\|^2 d\tau\right]^{1/2} \left[\int_{t_0}^{t} \|e(\tau)\|^2 d\tau\right]^{1/2}\end{aligned}$$

where the Schwartz inequality has been used, and $x_0 = x(t_0)$. Considering the limit as t tends to infinity and denoting with $\|\cdot\|_2$ the $\mathcal{L}_2$ norm, one has

$$\begin{aligned}V_o\,|_{\infty,x} - V_o\,|_{t_0,x_0} &\leq -\lambda_{\min}^Q \|e\|_2^2 + \Delta\|\phi\|_2\|e\|_2 \\ &\leq -\lambda_{\min}^Q \|e\|_2^2 + \Delta\ell_\phi\|e\|_2\end{aligned} \tag{21}$$

since, as observed, ϕ goes to zero exponentially, so that

$$\|\phi\|_2 = \ell_\phi < \infty$$

with ℓ_ϕ a constant. Therefore, since $V_o\,|_{\infty,x} \geq 0$

$$\lambda_{\min}^Q \|e\|_2^2 - \Delta\ell_\phi\|e\|_2 \leq V_o\,|_{t_0,x_0} - V_o\,|_{\infty,x} \leq V_o\,|_{t_0,x_0} \tag{22}$$

$$\|e\|_2^2 \leq \frac{\Delta\ell_\phi}{2\lambda_{\min}^Q} + \frac{1}{\sqrt{\lambda_{\min}^Q}} \left[V_o\,|_{t_0,x_0} + \frac{\Delta^2\ell_\phi^2}{4\lambda_{\min}^Q}\right]^{1/2}.$$

Hence, e is $\mathcal{L}_2$. Moreover, e is also bounded

The applications of Barbalat's theorem allows concluding that $\lim_{t\to x_0} e = 0$ i.e. this observer ensures the exponential convergence of the estimates $\hat{x}_1, \hat{x}_2$ to the states variables x_1, x_2 respectively. Hence, the error system in (14) has the origin exponentially stable, and the estimation errors tend exponentially to zero, with a time constant $\tau = 1/\lambda$.

4. EXPERIMENTAL RESULTS

To investigate the performance of the proposed nonlinear observer, a number of computer-simulated dynamic responses are obtained. Furthermore, the simulated designs are built and used in the real-time experiments on the dynamic test stand. All the following figures show experimental results for a car with an initial longitudinal velocity $V = 60km/h$ maneuvering on a straight line.

For the experiments for the nonlinear observer, there has to be a control signal, T_b, applied to the ABS Laboratory setup. For this work the control signal is obtained by a Control Lyapunov Function (Martinez-Gardea et al. (2014)). This strategy is a generalization of the notion of Lyapunov function used in the stability analysis of systems that uses the information of a Lyapunov function for the construction of the control law. An advantage of this technique is its extreme simplicity and ease of implementation, moreover, it automatically provides an analytic feedback law (Sontag (1989)). Nonetheless, the nonlinear observer could be implemented with any control input.

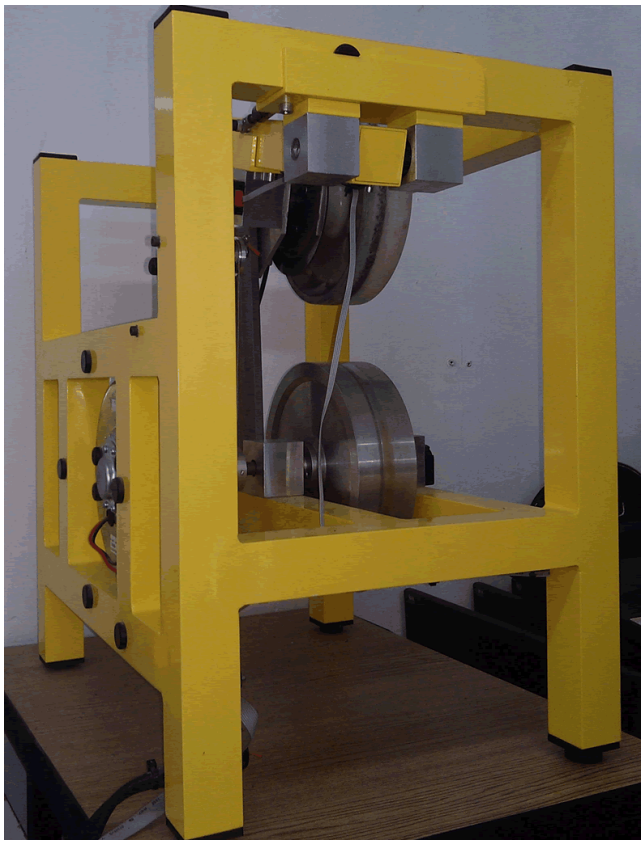

Fig. 4. Physical system of the ABS Laboratory setup.

In this section, the nonlinear observer's behavior is presented for the experimental platform of the ABS Laboratory setup. In Fig. 4 the physical system is shown, it simulates an ABS system. The upper wheel simulates the vehicle's wheel dynamics, and the lower wheel simulates the vehicle longitudinal velocity.

Model parameters and the nominal parameters used in this work, are described in Table 1, emphasizing the observer values k_{o1}, k_{o2} used in simulation and real time implementation.

4.1 Description of the graphics

In order to test the observer's behavior in the braking process, the system's upper wheel needs to reach an angular velocity of 1509 *rpm* or 158 *rad/seg* (that will be considered the initial condition of the system). After achieving this velocity the acceleration signal is deactivated and the braking process begins. The observer starts with a different initial condition for the angular velocity, in this

Table 1. Coefficients and System Variables, ABS Laboratory setup

r_1	0.0995 m
r_2	0.0990 m
J_1	7.54×10^{-3} Kg m^2
J_2	25.6×10^{-3} Kg m^2
d_1	118.74×10^{-6} Kg m^2/s
d_2	214.68×10^{-6} Kg m^2/s
M_{10}	0.0032 N m
M_{20}	0.0925 N m
c_{31}	20.34 s^{-1}
b_1	15.24
b_2	−6.21
D_x	22.99
C_x	1.15
B_x	28
k_{o1}	10
k_{o2}	40

case 1425 *rpm* or 150 *rad/seg*. This is done to show, that despite different initial conditions, the observer is capable of tracking the reference correctly. At the end of the braking process, when the velocity is near zero, the braking control is disabled because it is no longer effective therefore all the brake torque must be applied.

In Fig. 5 the real and estimated angular velocity of the upper wheel (that represents the wheel of the vehicle) are shown. In the same manner, Fig. 7 depicts the real and estimated angular velocity of the lower wheel (that represents the road surface dynamics). Both figures describe the good reference tracking accomplished by the observer despite the different initial conditions.

In Fig. 6 the estimation error defined in (12) of the real and estimated angular velocity of the upper wheel is shown. In Fig. 8 the estimation error, also defined in (12) of the real and estimated angular velocity of the lower wheel is shown. Both errors are bounded and small enough to display the observer's good behavior.

Fig. 9 shows the wheel slip, λ, obtained from the system defined in (3) and the wheel slip estimated, $\hat{\lambda}$, as in (11), that is evaluated through the nonlinear observer and the similarities between the two graphics are depicted. The difference between the real wheel slip and the estimation is small, when x_2 is approaching to zero λ increases and so does $\hat{\lambda}$, but the estimation error remains small.

Fig. 10 shows the road friction force, F_x, defined in (2), and the estimated road friction force, $\hat{F}_x$, as in (10), which are very much alike, additionally the error between these two forces, (19), is depicted in Fig. 11.

5. CONCLUSIONS

A series of experiments have been conducted to determine the performance of the proposed controller for different cases and conditions. For the experiments, the ABS Laboratory setup of Inteco Ltd. is used (Inteco (2006)). To imitate the behavior of the vehicle during braking on a dry and straight road, the wheel is accelerated until the velocity of the wheel reaches 60 km/h. Once it attains the limit velocity, the braking operation begins. There is another velocity threshold which states the minimum velocity level for applying ABS control algorithms. Under this

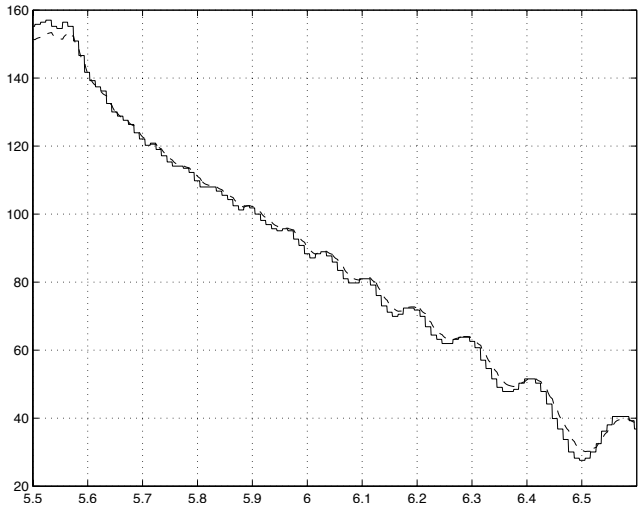

Fig. 5. Upper wheel's angular velocity real time measurement x_1 (solid) vs upper wheel estimated angular velocity $\hat{x}_1$ (dotted) [rad/seg].

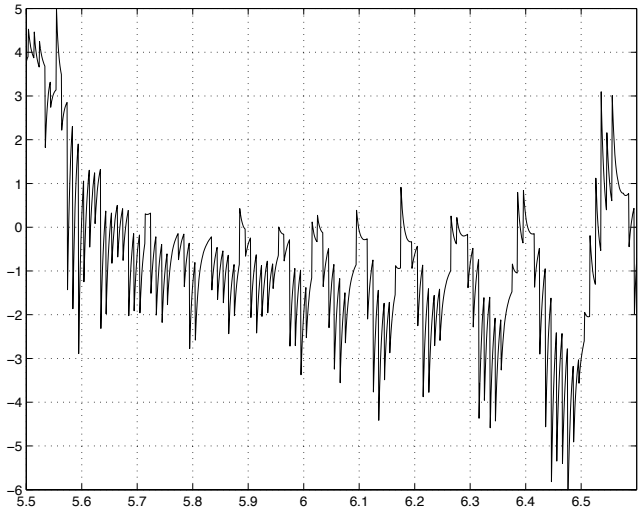

Fig. 6. Upper wheel angular velocity, error estimation $e_1 = x_1 - \hat{x}_1$.

minimum value of velocity, the system becomes unstable if the ABS algorithm is applied. Under such circumstance, the maximum braking torque should be applied to the wheels, without considering the target slip value.

This work proposes a nonlinear observer in order to estimate the angular velocity of the lower wheel of the ABS Laboratory setup, by Inteco Ltd. This wheel represents the road surface, so it provides information about longitudinal displacement and longitudinal velocity. The observer design is based on the available angular velocity of the upper wheel (which represents the vehicle's wheel), the static friction disturbances are also known, and the proposed control input is based on the CLF technique. A mathematical analysis to demonstrate the stability of the system is done, and a stability region for the observer is obtained. The performance of the observer was proved in both; computer simulations, and real time tests, the results show a good performance of the observer, correctly tracking the reference and with small and bounded errors.

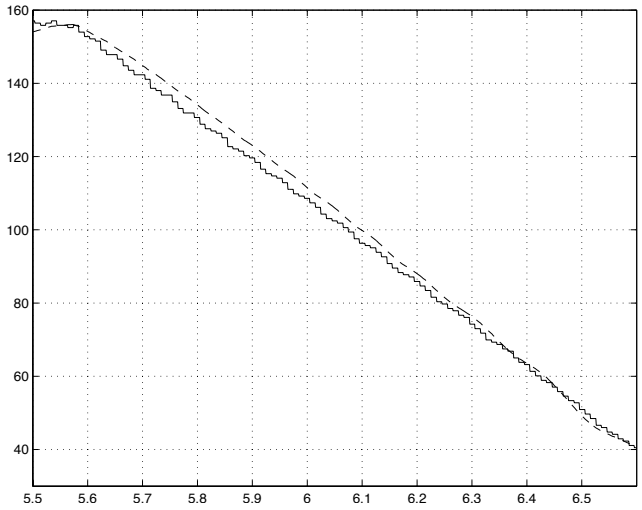

Fig. 7. Lower wheel's angular velocity real time measurement x_2 (solid) vs lower wheel estimated angular velocity $\hat{x}_2$ (dotted) [rad/seg].

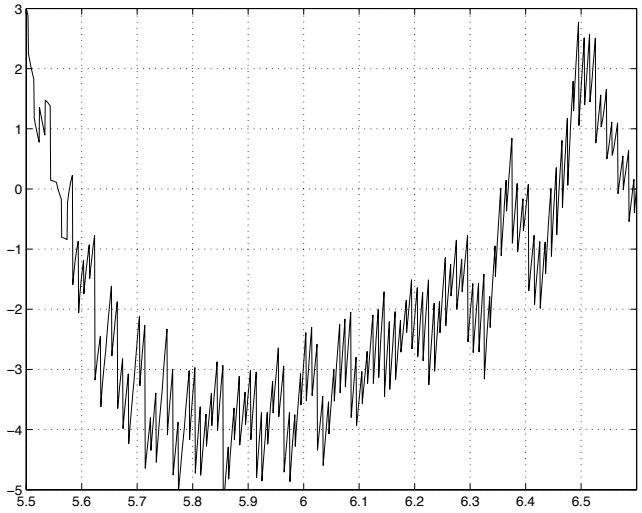

Fig. 8. Lower wheel angular velocity, error estimation $e_2 = x_2 - \hat{x}_2$.

ACKNOWLEDGEMENTS

The authors acknowledge Enrique Villasana for the help in the realization of the simulations.

The authors would like to thank Universidad de Guadalajara – Centro Universitario de la Ciénega, especially to the Master and Doctoral Departments.

Research supported by CONACYT scholarship 513153.

REFERENCES

Al-Mola, M., Mailah, M., Samin, P., Muhaimin, A., and Abdullah, M. (2014). Performance comparison between sliding mode control and active force control for a nonlinear anti-lock brake system. *WSEAS Trans. on Systems and Control*, 9, 101–107.

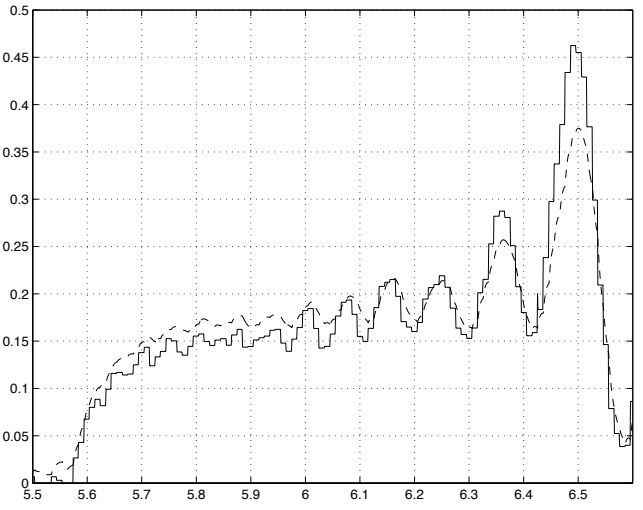

Fig. 9. Real wheel slip λ (solid) vs estimated wheel slip $\hat{\lambda}$ (dotted).

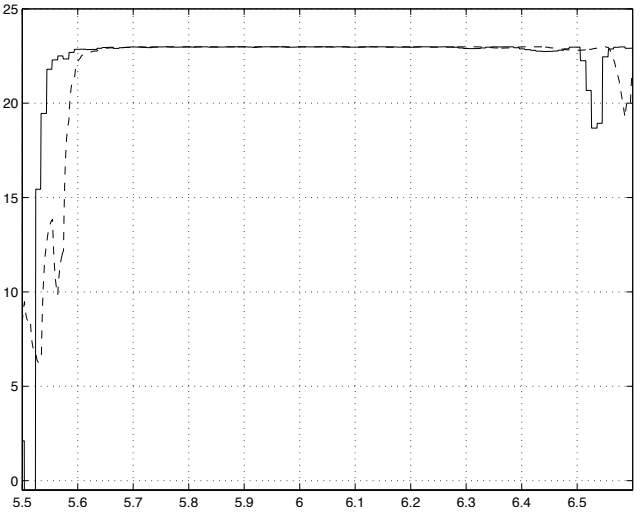

Fig. 10. Road friction force F_x (solid) vs estimated road friction force $\hat{F}_x$ (dotted) [N-m].

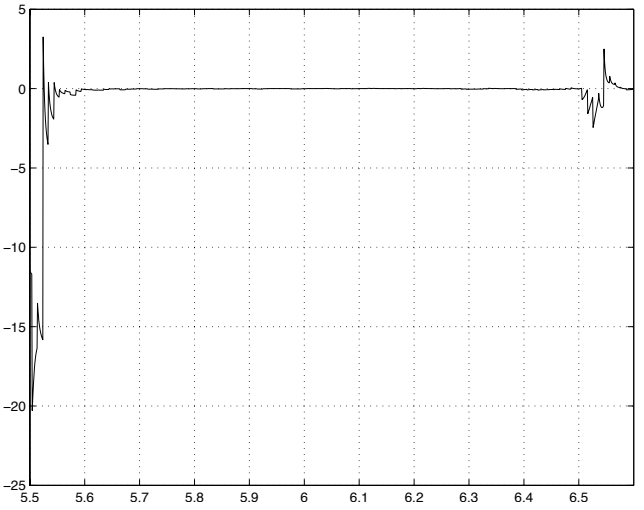

Fig. 11. Road friction force estimated error $F_x - \hat{F}_x$ [N-m].

Baffet, G., Stephant, J., and Charara, A. (2007). Lateral vehicle dynamic observers: simulations and experiments. *International Journal of Vehicle Autonomous Systems*, 5(3-4), 184–203.

Bosch GmbH, R. (2003). `http://www.bosch.com/`.

Cabrera, J., Ortiz, A., Castillo, J., and Simon, A. (2005). A fuzzy logic control for antilock braking system integrated in the imma tire test bench. *Vehicular Technology, IEEE Transactions on*, 54(6), 1937–1949. doi: 10.1109/TVT.2005.853479.

Chen, G., Wang, W., Lee, T., and Tao, C. (2006). Observer-based direct adaptive fuzzy-neural control for anti-lock braking systems. *International Journal of Fuzzy Systems*, 8(4).

Dadashnialehi, A., Bab-Hadiashar, A., Cao, Z., and Kapoor, A. (2012). Accurate wheel speed measurement for sensorless abs in electric vehicle. In *Vehicular Electronics and Safety (ICVES), 2012 IEEE International Conference on*, 37–42. doi:10.1109/ICVES.2012.6294313.

Dadashnialehi, A., Bab-Hadiashar, A., Cao, Z., and Kapoor, A. (2014). Intelligent sensorless abs for in-wheel electric vehicles. *Industrial Electronics, IEEE Transactions on*, 61(4), 1957–1969. doi:10.1109/TIE.2013.2266085.

DaimlerAG (2008). Mercedes-benz and the invention of the anti-lock braking system: Abs, ready for production. `http://media.daimler.com/`.

Emig, R., Goebels, H., and Schramm, J. (1990). Antilock braking systems (abs) for commercial vehicles - status 1990 and future prospects. In *Transportation Electronics, 1990. Vehicle Electronics in the 90's: Proceedings of the International Congress on*, 515–523. doi:10.1109/ICTE.1990.713050.

Habibi, M. and Yazdizadeh, A. (2010). A new fuzzy logic road detector for antilock braking system application. In *Control and Automation (ICCA), 2010 8th IEEE International Conference on*, 1036–1041. doi:10.1109/ICCA.2010.5524203.

Imsland, L., Grip, H., Johansen, T., Fossen, T., Kalkkuhi, J., and Suissa, A. (2007). Nonlinear observer for vehicle velocity with friction and road bank angle adaptation - validation and comparison with an extended kalman filter. In *SAE World Congress and Exhibition*.

Inteco, L. (2006). *Inteco Ltd, The Laboratory Antilock Braking System controlled from PC, User Manual*. Poland.

John, S. and Pedro, J. (2009). A comparative study of two control schemes for anti-lock braking systems. In *2009 Control Conference (ASCC), 9th Asian*.

Kayacan, E., Oniz, Y., and Kaynak, O. (2009). A grey system modeling approach for sliding-mode control of antilock braking system. *Industrial Electronics, IEEE Transactions on*, 56(8), 3244–3252. doi:10.1109/TIE.2009.2023098.

Khanesar, M., Kayacan, E., Teshnehlab, M., and Kaynak, O. (2012). Extended kalman filter based learning algorithm for type-2 fuzzy logic systems and its experimental evaluation. *Industrial Electronics, IEEE Transactions on*, 59(11), 4443–4455. doi:10.1109/TIE.2011.2151822.

Kiencke, U. and Nielsen, L. (2010). *Automotive control systems: For engine, driveline and vehicle*. Springer, 2nd edition.

Martinez-Gardea, M., Mares Guzman, I., Di Gennaro, S., and Acosta Lua, C. (2014). Experimental comparison of linear and nonlinear controllers applied to an antilock braking system. In *Control Applications (CCA), 2014 IEEE Conference on*, 71–76. doi:10.1109/CCA.2014.6981331.

Oniz, Y., Kayacan, E., and Kaynak, O. (2009). A dynamic method to forecast the wheel slip for antilock braking system and its experimental evaluation. *IEEE Transaction on System, Man and Cybernetics–Part B: Cybernetics*, 39(2).

Pacejka, H. (2006). *Tyre and Vehicle Dynamic*. Elseiver, 2nd edition.

Petrov, M., Balankin, V., and Naruzhnyi, O. (1977). Study of automobiles brakes and pneumatic tires work model of the work process of antilock brake system. NISI, Tech.

Precup, R., Spataru, S., Radac, M., Petriu, E., Preitl, S., and Dragos, C. (2010a). Model-based fuzzy control solutions for a laboratory antilock braking system. In *Human System Interactions (HSI), 2010 3rd Conference on*, 133–138.

Precup, R., Spataru, S., Radac, M., Petriu, E., Preitl, S., and Dragos, C. (2010b). Stable and optimal fuzzy control of a laboratory antilock braking system. In *Advanced Intelligent Mechatronics (AIM), 2010 IEEE/ASME International Conference on*, 593–598. doi:10.1109/AIM.2010.5695728.

Precup, R., Spataru, S., Radac, M., Petriu, E., Preitl, S., Dragos, C., and David, R. (2012). Experimental results of model-based fuzzy control solutions for a laboratory antilock braking system. In *Human Computer Systems Interaction: Backgrounds and Applications 2*, volume 99, 223–234. doi:10.1007/978-3-642-23172-8_16.

Rajamani, R. (2011). *Vehicle dynamics and control*. Springer, 1st edition.

Rittmannsberger, N. (1998). Antilock braking system and traction control. In *Proc. of Int. Congress on Transportation Electronics Convergence*, 195–202.

Sontag, E.D. (1989). A universal construction of artstein's theorem on nonlinear stabilization. *Systems and Control Letters*, 13, 117–123.

Stephant, J., Charara, A., and Meizel, D. (2007). Evaluation of sliding mode observer for vehicle sideslip angle. *Control Engineering Practice*, 15, 803–812.

Topalov, A., Kayacan, E., Oniz, Y., and Kaynak, O. (2009a). Adaptive neuro-fuzzy control with sliding mode learning algorithm: Application to antilock braking system. In *Asian Control Conference, 2009. ASCC 2009. 7th*, 784–789.

Topalov, A., Kayacan, E., Oniz, Y., and Kaynak, O. (2009b). Neuro-fuzzy control of antilock braking system using variable-structure-systems-based learning algorithm. In *Adaptive and Intelligent Systems, 2009. ICAIS '09. International Conference on*, 166–171.

Topalov, A., Oniz, Y., Kayacan, E., and Kaynak, O. (2011). Neuro-fuzzy control of antilock braking system using sliding mode incremental learning algorithm. *Neurocomputing*, 74(11), 1883–1893.

Zhao, L., Liu, Z., and Chen, H. (2011). Design of a nonlinear observer for vehicle velocity estimation and experiments. *Control Systems Technology, IEEE Transactions on*, 19(3), 664–672. doi:10.1109/TCST.2010.2043104.